User Support Office use only

Date: October 18, 2011

Proposal for Nuclear Physics Experiment at RI Beam Factory

(RIBF NP-PAC-10, 2011)

Title of Experiment	MINOS (ミノス): a H_2 target and vertex-tracker device for in-beam gamma spectroscopy at relativistic energies.
Category	[ ] NP experiment [ ] Detector R&D [X] Construction [ ] Update proposal (Experimental Program: NP_____– _____)
Experimental Device	[ ] GARIS [ ] RIPS [ ] BigRIPS [ ] Zero Degree [ ] SHARAQ [ ] SAMURAI
Detector	[ ] DALI2 [ ] GRAPE [ ] EURICA

Spokesperson :

Name	OBERTELLI Alexandre		
Institution	CEA Saclay		
Title of position	researcher		
Address	CEA Saclay, SPhN, Orme des Merisiers, building 703, 91191 Gif-sur-Yvette, France		
Tel	+33 1 69 08 75 55	Fax	+33 1 69 08 75 84
Email	alexandre.obertelli@cea.fr		

Beam Time Request Summary:

Tuning with beam	Days
DATA RUNS	Days
TOTAL	**Days**

Primary Beam:

Particle		Energy	(*A* MeV)	Intensity	

RI Beams			Beam-On-Target Time for DATA RUN
Isotope	Energy(*A*MeV)	Intensity(/s)	Days

Your proposal should be sent to User Support Office (UserSupportOffice@ribf.riken.jp)

Summary:

In-flight gamma spectroscopy of rare isotopes at relativistic energies, from fifty to several hundreds of MeV/nucleon, is one of the most efficient tools to investigate shell effects in exotic nuclei. We propose a new method leading to an increased sensitivity for prompt-gamma spectroscopy.

The intended program is based on proton-induced knockout reactions such as *(p,2p)* and *(p,pn)* at RIBF using the DALI2 setup. The new device MINOS consists of a thick liquid hydrogen target surrounded by a cylindrical Time Projection Chamber, playing the role of a vertex tracker. MINOS will allow the use of a thick target, and therefore increased luminosity, while maintaining good Doppler-reconstruction capabilities. MINOS has been funded by the European Research Council for the 2010-2015 period.

We believe that the coupling of DALI2 and MINOS will bring new opportunities to investigate nuclear structure far away from stability at RIKEN/RIBF.

List of Collaborators

Name	Institution	Title or position	Email
N. Alamanos	CEA Saclay	Research director	nicolas.alamanos@cea.fr
S. Anvar	CEA Saclay	Senior engineer	shebli.anvar@cea.fr
N. Aoi	RCNP	Researcher	aoi@rcnp.osaka-u.ac.jp
L. Audirac	CEA Saclay	Postdoc	laurent.audirac@cea.fr
G. Authelet	CEA Saclay	Technician	gilles.authelet@cea.fr
H. Baba	RIKEN	Researcher	baba@ribf.riken.jp
P. Bargueden	CEA Saclay	Technician	patrick.bargueden@cea.fr
S. Boissinot	CEA Saclay	PhD student	simon.boissinot@cea.fr
D. Calvet	CEA Saclay	Engineer	denis.calvet@cea.fr
A. Corsi	CEA Saclay	Postdoc	acorsi@cea.fr
A. Delbart	CEA Saclay	Engineer	alain.delbart@cea.fr
E. Delagnes	CEA Saclay	Senior engineer	eric.delagnes@cea.fr
P. Doornenbal	RIKEN	Postdoc	pieter@ribf.riken.jp
F. Druillole	CEA Saclay	Engineer	frederic.druillole@cea.fr
R. Durand	CEA Saclay	Technician	robert.durand@cea.fr
J.-M. Gheller	CEA Saclay	Engineer	jean-marc.gheller@©ea.fr
A. Giganon	CEA Saclay	Technician	arnaud.giganon@cea.fr
A. Gillibert	CEA Saclay	Senior researcher	alain.gillibert@cea.fr
P. Guiho	CEA Saclay	Technician	patrice.guiho@cea.fr
J-M Joubert	CEA Saclay	Technician	jean-michel.joubert@cea.fr
D. Khoa	INST, Hanoi	Senior researcher	khoa@vaec.gov.vn
W. Korten	CEA Saclay	Senior researcher	wolfram.korten@cea.fr
C. Lahonde-Hamdoun	CEA Saclay	Technician	caroline.lahonde-hamdoun@cea.fr

V. Lapoux	CEA Saclay	Researcher	valerie.lapoux@cea.fr
D. Leboeuf	CEA Saclay	Engineer	didier.leboeuf@cea.fr
K. C. Lee	INST, Hanoi	Researcher	chungxl@yahoo.com
J. Lee	RIKEN	Researcher	jennylee@ribf.riken.jp
C. Louchart	CEA Saclay	PhD student	corinne.louchart@cea.fr
A. Mohamed	CEA Saclay	Technician	azath.mohamed@cea.fr
J.-P. Mols	CEA Saclay	Technician	jean-philippe.mols@cea.fr
T. Motobayashi	RIKEN	Senior researcher	motobaya@riken.jp
M. Nishimura	RIKEN	Researcher	mizuki@riken.jp
A. Obertelli	CEA Saclay	Researcher	alexandre.obertelli@cea.fr
H. Otsu	RIKEN	Researcher	otsu@ribf.riken.jp
E. Pollacco	CEA Saclay	Senior researcher	emmanuel.pollacco@cea.fr
G. Prono	CEA Saclay	Technician	gilles.prono@cea.fr
J.-Y. Rousse	CEA Saclay	Engineer	jean-yves.rousse@cea.fr
A. Roger	CEA Saclay	Technician	arnaud.roger@cea.fr
S. Takeuchi	RIKEN	Researcher	takesato@riken.jp
K. N. Tuan	INST, Hanoi	Researcher	ntkhai@iop.vast.ac.vn
T. Uesaka	RIKEN	Senior researcher	uesaka@riken.jp
K. Yoneda	RIKEN	Researcher	yoneda@ribf.riken.jp

MINOS: a H_2 target and vertex tracker device for in-beam gamma spectroscopy at relativistic energies

L. Audirac, D. Calvet, A. Corsi, A. Delbart (technical project leader),
J.-M. Gheller, A. Gillibert, V. Lapoux, C. Louchart,
D. Leboeuf, A. Obertelli (scientific project leader), E. Pollacco
CEA Saclay, IRFU, 91191 Gif-sur-Yvette, France

H. Baba, P. Doornenbal, J. Lee, T. Motobayashi, M. Nishimura,
H. Otsu, S. Takeuchi, T. Uesaka, K. Yoneda
RIKEN Nishina center, Saitama 351-0198, Japan

N. Aoi
RCNP, Osaka, Japan

October 19, 2011

Contents

1 Context

Atomic nuclei are few-body systems, mainly governed by the strong force, and by quantum mechanical laws leading to a shell structure for the nucleons. Shell gaps represent the backbone of nuclear structure and are a direct fingerprint of the nucleon-nucleon interaction. Magic nuclei, with a magic number of protons and neutrons, are spherical and more inert that their neighbors since their excitation requires more energy to scatter nucleons above the energy gap to reach the next shell. Magic numbers are well established for stable nuclei: 2, 8, 20, 28, 50, 82, 126 but are known not to be universal over the nuclear chart. Indeed, the nuclear shell structure is known to change, sometimes drastically, with the number of protons and neutrons, revealing how delicate is the arrangement of nucleons in interaction. The study of unstable nuclei out of the valley of stability is the only way to establish the structure of nuclei throughout the nuclear chart and unravel the isospin properties of the nuclear force. New shell closures or strong shell reordering are predicted in regions which may be difficult to explore, due to the limit in the curents setups and to the beam intensties. More specifically, the N=20 and N=28 shell gaps are known to vanish for neutron-rich nuclei but these phenomena still need further investigation, the Z = 28 shell closure is claimed to weaken in the region of the (not so?) doubly magic ^{78}Ni and stabilizing shell effects are predicted at N = 34, N = 70 in ^{54}Ca and ^{110}Zr, respectively. Finally, a recent experiment indicated a new island of inversion, i.e. a region in which orbits are lowered in energy from the upper shell into the active shell due to deformation, in neutron-rich N = 40 nuclei, in contradiction with some model predictions. All these effects originate in the properties of the in-medium nucleon-nucleon interaction [1, 2] and possibly, as argued recently, in the 3N forces coming from the composite structure of the nucleons [3, 4]. The fundamental question of the nuclear force and the assessment of increased-stability regions in the neutron-rich part of the nuclear landscape are of prior importance for a better understanding of the r-process path during core collapses of supernovae and the stellar nucleosynthesis in the Universe. Such studies should contribute to solve the problem of the origin of the heaviest elements from Fe to U in nature.

Different observables, such as the nuclear mass or the excitation energy of the first excited state, can be used to characterize nuclear shell gaps. In even-even nuclei, the excitation energy of the first excited 2^+ state, in most cases the first excited state, is very sensitive to the shell structure above the Fermi level. Large 2^+-state excitation energies directly correspond to large energy shell gaps. Conversely, small excitation energies correspond to collective nuclei with, apart from few exceptions, a large transition probability B(E2;$0^+ \rightarrow 2^+$). Experimentally, the spectroscopy of the most exotic isotopes has been reached, in many cases, via prompt gamma spectroscopy from secondary reactions of exotic beams produced by fragmentation at intermediate energy. The excitation energy of the first excited state in even-even nuclei is a direct measurement of the orbit density above the Fermi level: magic nuclei's first excited state presents a large excitation energy intimately linked to the considered energy gap. Worldwide, four laboratories are using this technique (GANIL in France, GSI in Germany, NSCL in USA and RIKEN in Japan) and have recently provided, for instance, the first spectroscopy of ^{42}Si [5], ^{36}Mg [6] or ^{32}Ne [7], all leading to new and crucial experimental information concerning shell-structure or shape evolution with isospin. Among these laboratories, the new upgraded laboratory of RIKEN [9] in Japan and the future FAIR facility [8] in Europe will share in the next 10 years the leadership in producing very exotic nuclei at energies above 200 MeV/nucleon. Nucleon knockout reactions coupled to gamma-detection arrays have indeed been demonstrated to be very efficient to populate the most exotic species and perform their prompt gamma-decay spectroscopy [10]. Up to now, this method is based on the coupling of a gamma spectrometer (Germanium arrays such as RISING at GSI or scintillator arrays such as DALI2 at

RIKEN) around a heavy-ion target, ^{12}C or ^{9}Be usually, and an identification device for the projectile-like fragment (e.g. the S800 magnetic spectrometer at the NSCL, the zero-degree spectrometer at RIKEN or the new LYCCA0 implantation array at GSI). The γ rays are detected in coincidence with a knockout residue, identified in mass and atomic charge by the above-mentioned recoil detector. The measured energy E_γ is corrected from the Doppler shift due to in flight emission, following the relation

$$E_0 = E_\gamma \frac{1 - \beta \cos(\theta)}{\sqrt{1 - \beta^2}} \quad (1)$$

where E_0 is the nuclear transition energy in the nucleus frame, β is the velocity of the ejectiles when the transition is emitted and θ is the angle defined by the ejectiles velocity and the emitted gamma ray direction. The power of a gamma-ray detection setup for intermediate-energy studies, in addition to its geometrical efficiency, is directly related to its capability to perform a good Doppler correction. This depends on (i) the angle of the photon relative to the scattering angle of the residue, strongly related to the gamma detector granularity, and (ii) the velocity of the ejectile when emitting the photon. This last point, for prompt decays, is related to the energy loss of the beam and the resulting velocity spread inside the target. For a given beam intensity, all existing setups are therefore limited by the same parameters: (i) the energy- and position-resolution and efficiency characteristics of the gamma spectrometer. This limitation will be soon largely reduced by new-generation high-resolution 4-π gamma arrays, such as the European AGATA spectrometer, composed of 180 Germanium detectors (60 clusters) with a 4-mm position resolution for the first-interaction position, based on the gamma-tracking method. Compared to existing arrays, the gain in sensitivity due to AGATA can reach 20 in case of low-multiplicity intermediate-energy studies. The one-π configuration is expected at GSI for an experimental campaign in 2014. The American detector GRETA will have similar characteristics. (ii) The choice of the target is a compromise between a thick target to increase the luminosity and a thin target to increase the sensitivity of the detection by minimizing the energy loss, and therefore the velocity spread, in the target and for a better Doppler-effect correction. Indeed, up to now in prompt gamma spectroscopy, one does not have access to the velocity of the fragment when it emits the photon from the inside of the target.

In that environment, the European Research Council (ERC) allocated a research grant to the MINOS project for the 2010-2015 period. This project, based on a novel experimental setup, is dedicated to in-beam gamma spectroscopy at relativistic energies at RIKEN and, in a later future, is intended to be also used at FAIR.

In the MINOS program, we propose to develop a new experimental technique by using nucleon-removal from very exotic nuclei on a very thick liquid hydrogen target coupled to a proton tracker that aims at measuring, on an event-by-event basis, the reaction-vertex position in the target. The device can be considered as an active target. By measuring this vertex, one allows the use of target of hundreds of millimeters with improved detection sensitivity, i.e. the Doppler correction is better than with a passive heavy-ion target. The only remaining limiting factor is that one has to ensure that the second-interaction probability in the target is low since the knockout fragment has to be identified after the target. For incident energies of 200-400 mega electron-volt per nucleon (MeV/nucleon), a typical length of 150 mm allows to respect this condition. This development will induce a unique gain in detection sensitivity of more than an order of magnitude compared to experiments with solid heavy-ion targets in some cases, allowing the detailed spectroscopy of nuclei produced at less than 1 particle per second and leading to the potential discovery of new shell effects, further inside the Terra Incognita of the nuclear landscape. **The device is expected to be ready for physics experiments at the end of 2013.**

The coupling of the DALI2 spectrometer and the MINOS device is expected to provide unique opportunities for the study of very exotic nuclei at RIBF. In comparison with usual inclusive heavy-ion induced knockout reactions, the expected advantages are

- **Higher statistics**: through the vertex tracker, the target thickness (atom.cm^{-2}) that one could use for gamma spectroscopy exceeds a factor of 5 compared to standard targets.
- **Better resolution**: a 3-mm FWHM precision in determining the reaction vertex position is equivalent, in terms of velocity undetermination, to the use of a 300-μm thick ^{9}Be target. It entails a cancellation of the β-uncertainty component in the energy resolution in the final Doppler-corrected energy spectrum (see Fig. 1 for the energy resolution components with DALI2). Note that this gain will be very high in case of the use of high-resolution gamma arrays with high granularity such as the new-generation gamma detectors GRETA and AGATA.
- **More sensitive** to spectroscopic information: (i) the distribution of the relative angle between the two emitted protons in (p,2p) reactions give a precise information on the intrinsic ℓ momentum of the removed nucleon. (ii) By an exclusive measurement (proton detection), we expect to better control the direct part of the reaction-mechanism process and extract reliable spectroscopic factors from the measure data.

In the following section, we present the core physics programme of MINOS and highlight possible experiments that could be performed once the required beam intensities are available at RIBF. Section 3 is devoted to the technical description of the MINOS device, including electronics and simulations. The foreseen implementation at RIKEN is detailed in section 4. Finally, we present the current agenda of the project in section 5 as of today.

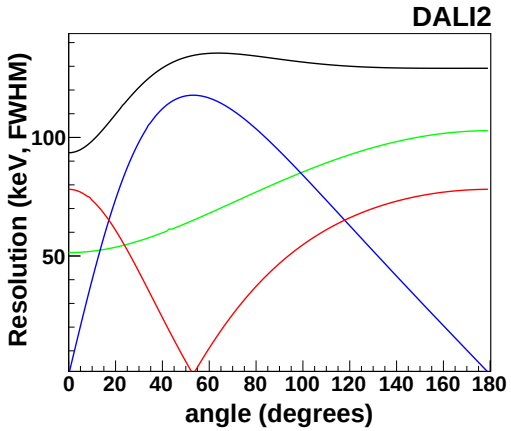

Figure 1: Energy resolution obtained with DALI2 as a function of the detection angles of the gamma ray (1 MeV in the emitting-nucleus frame). The resolution is calculated for a velocity β=0.6 and a velocity spread in the target of $\delta\beta$=0.05. A mean opening angle of the DALI2 detectors of 9° has been considered. The intrinsic energy resolution has been taken as $2.3 \times \sqrt{E_\gamma}$ keV, with E_γ in keV. The different origins of the resolution are shown: intrinsic resolution (green), $\delta\beta$ dependence (red) and angular uncertainty (blue). The total resolution is taken as the quadratic sum of all components (black).

2 Physics cases

During the period covered by this proposal, we will focus on the shell structure of medium mass nuclei, currently under debate. The key experiments targeted by MINOS are hardly doable today with existing setup and facilities. The proposed setup will be extremely competitive to achieve the physics objectives. We propose to investigate the existence of new shell-closures, or strong stabilizing shell effects, at N = 34, 40, 70 in ^{54}Ca, ^{60}Ca, ^{110}Zr, or constrain the robustness of Z = 28 and N = 50 in ^{78}Ni. More precisely, the following questions will be examined:

- Does N = 34 become a sub-shell closure at the neutron drip line? Is ^{54}Ca doubly magic as pointed out by state-of-the-art shell-model calculations?
- Is there a new island of inversion at N = 40 when one reaches ^{62}Ti as recently states or, on the contrary, is N = 40 a new sub-shell closure at ^{60}Ca?
- How strong are the Z = 28 and N = 50 shell closures as one reaches very neutron-rich nuclei? Is ^{78}Ni a doubly-closed shell nucleus?
- Is there a shell stabilization at N=70 at ^{110}Zr, originating in the quenching of the N=82 shell closure? Would this stabilization be strong enough to explain the deficiency of most models to explain matter abundance prior the A = 130 peak in the r-process pattern?

To tackle these questions, we propose to perform the spectroscopy of the mentioned nuclei and neighboring nuclei via $(p, 2p)$-type reactions at RIKEN with the DALI2 γ spectrometer coupled to the zero-degree spectrometer or the Samurai spectrometer for the detection of projectile-like residues. During the experiments, the secondary beam will be separated with the BigRips spectrometer [9]. Identification of incoming particles and fragments will be unambiguously achieved. The use of SAMURAI should offer the advantage of a large momentum acceptance, allowing to measure several reaction channels at the same time ($(p, 2p)$, (p, pn) and $(p, 3p)$ for example) with a mass resolution of about 1/100. In the case of the zero-degree spectrometer, a better mass resolution could be achieved allowing to perform experiments with heavy nuclei within the r-process path.

2.1 The N=34 new shell closure: spectroscopy around ^{54}Ca

Shell-model calculations with the GXPF1 interaction indicated an energy gap at N = 34, arising from a large energy spacing between the neutron $p_{1/2}$ orbital and the higher $f_{5/2}$ orbital, that should appear already at Z = 22 (Titanium isotopes) [11]. This prediction was not confirmed by the experimental data on the yrast structure of the N = 34 nuclei ^{56}Ti [12] and is contested by other shell-model interactions and mean-field predictions [13, 14]. This last point has been interpreted as the result of the strong $\pi f_{7/2}$-$\nu f_{5/2}$ monopole interaction that would bring the $\nu f_{5/2}$ and $\nu p_{1/2}$ orbits closer in energy, hindering the formation of the N = 34 subshell gap. It might be that in the GXPF1 interaction the effect of adding two protons to Calcium (Z=22) has been underestimated. In the calcium isotopes, the removal of the last two protons from the $\pi f_{7/2}$ might result in a shift of the $\nu f_{5/2}$ orbit, resulting in a larger gap in the single-particle energies between the $\nu p_{1/2}$ and the $\nu f_{5/2}$. This would lead to a subshell closure in N = 34. Recent *ab initio* studies suggest that the 3-body force plays a crucial role in explaining shell closures with a very impact on the magicity of ^{54}Ca [4]. Its most direct evidence would be a high excitation energy of the first 2^+ state in ^{54}Ca which represents a stringent constraint to establish the fp shell single-particle in the neutron-rich region around and beyond ^{54}Ca. This measurement is at reach at RIKEN with existing experimental

setups. We propose to further investigate this region, for example by performing the spectroscopy of ^{53}Ca from one neutron removal from ^{54}Ca and one proton removal from ^{54}Sc. Assuming a 20 pnA primary beam of ^{82}Se, we expect intensities of 2 pps of ^{54}Ca. With the same primary beam, an intensity of 34 pps of ^{54}Sc is estimated. The robustness of the subshell closure at $N = 34$, if any, could be studied via the spectroscopy of ^{52}Ar produced from ^{53}K(p,2p).

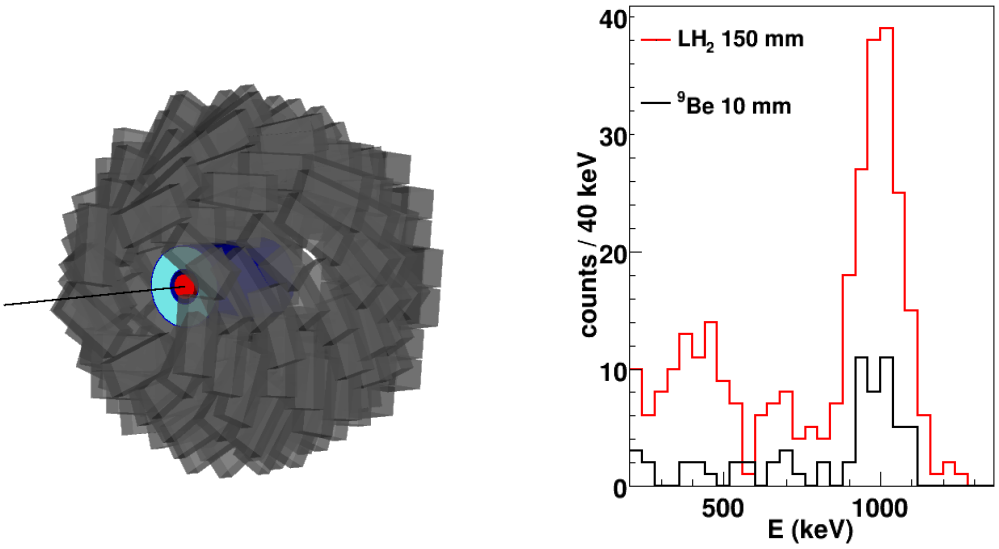

Figure 2: (Left) Geometry of ther DALI2+MINOS setup in Geant4. The H_2 target is drawn in red and the TPC in blue. (Right) Doppler-corrected gamma spectrum obtained for 150k impinging ^{53}K on the secondary target at 253 keV/nucleon (equivalent to 3 days of beam time at an intensity of 0.5 pps). Simulation for ^{53}K(p,2p)^{52}Ar are shown for a 150-mm hydrogen target and a 10-mm Be target. Statistics is obtained assuming a 5 mb cross section to populate the first 2^+ state (assumed here at 1 MeV) for both targets.

2.2 Shell inversion or new shell closure at N = 40: spectroscopy of ^{62}Ti and ^{60}Ca

The N=40 sub-shell closure has been actively investigated in the recent years, especially in the region of ^{68}Ni, both experimentally and theoretically. The excitation energy and the electromagnetic transition probability B(E2;$0^+ \rightarrow 2^+$) value of the first excited state of ^{68}Ni, when compared to those of neighboring Ni isotopes, suggest that the N = 40 gap between the νpf shell and the $\nu g_{9/2}$ orbital stabilizes the nucleus in a spherical shape. It has been suggested that N = 40 may be magic far away from stability [15], whereas other interpretation disputed this conclusion [16]. Experimentally, one does not observe a stabilizing effect from the fp-$g_{9/2}$ gap in other neutron-rich N = 40 nuclei, as can be seen in 2^+ energies of even-mass Fe isotopes. The systematic indicates a growing deformation when approaching N = 40, which is interpreted as the intrusion of the gd orbits towards the Fermi energy. The excitation energy of the first 2^+ state in Iron and Chromium isotopes has been measured up to ^{68}Fe and ^{62}Cr [17], respectively. The first 2^+ state of the N = 40 isotone ^{64}Cr has been recently measured at 420 MeV[18]. It has recently been claimed, from fragmentation cross section systematics, that a strong structure change occurs around ^{62}Ti and has been interpreted as a potential new island of inversion at ^{62}Ti. This could be due to the lowering of the $g_{9/2}$ orbital into the $pf_{5/2}$ region [19]. On the other hand, a recent collaboration [20] with mean-field theorists from CEA Bruyères-le-Châtel show another interpretation: as one moves along the N = 40 shell towards

the drip line, a maximum of collectivity is found for ^{64}Cr, whereas ^{62}Ti tends to be spherical since close to ^{60}Ca, predicted doubly magic. The situation is therefore controversial and needs further investigation. The spectroscopy of ^{62}Ti and ^{60}Ca is difficult to access and will benefit from the MINOS development. A ^{62}Ti beam predicted at 20 pps should be reached at RIKEN when an intense ^{82}Se beam of 100 pnA at 350 MeV/nucleon will be available, as planned. In that case, the first excited 2^+ state in ^{60}Ca could be reached via the two proton removal ^{62}Ti(p,3p)^{60}Ca. This measurement would status on the magicity of N = 40 along the Calcium chain.

2.3 The weakening of the Z=28 magic number in the region of ^{78}Ni

The spectroscopy of ^{78}Ni and of neighboring nuclei is of large importance for our understanding of nuclear structure since this nucleus is one of the very few unstable (expected) doubly magic nuclei that will be accessible with the new-generation machines. The Z=28 shell closure originates in the spin-orbit interaction. The erosion of this shell closure has been suggested from the comparison of experimental data to shell model calculations based on a ^{48}Ca core [21, 22]. Recently, the tensor term of the non central part of the nucleon-nucleon interaction has been proposed as a good candidate to explain the reduction of the Z=28 gap while filling the neutron $g_{9/2}$ orbit (i.e. towards ^{78}Ni) [23]. The detailed spectroscopy of ^{78}Ni and its neighbors nuclei is crucial to determine the single-particle of very neutron-rich nuclei. Indeed, if ^{78}Ni appears to be doubly magic, it could be used as a core for shell-model calculations for nuclei in the terra incognita, with protons in the fp shell and neutron above the $g_{9/2}$ orbit. Reliable predictions require the measurement of experimental single-particle energies in the vicinity of ^{78}Ni. The MINOS project should provide the necessary tools to access spectroscopic information in this region. Up to now, ^{80}Zn is the closest nucleus to ^{78}Ni whose spectroscopy has been performed [24]. The recent upgrades at RIKEN aim at a nominal ^{86}Kr beam intensity of 100 pnA at 350 MeV/nucleon. These nominal intensities are expected for 2013 and should result in a ^{80}Zn beam of 60 pps and a ^{79}Cu beam of 2.5 pps at energies of 300 MeV/nucleon. The first 2^+ state of ^{78}Ni could then be reached via ^{80}Zn(p,3p)^{78}Ni or ^{79}Cu(p,2p)^{78}Ni with the tracker/target device. Due to the low beam intensities, the sensitivity gains offered by the MINOS project should be decisive in measuring the excitation energy of ^{78}Ni(2^+) and the spectroscopy of neighboring nuclei.

2.4 Island of stability at N=70 for ^{110}Zr and the related quenching of N=82

The nucleus ^{110}Zr has been exhibited as a unique candidate whose structure may produce visible effects on the r-process nuclear abundance. According to several nuclear-structure models, this nucleus is strongly deformed in its ground state. If the N=82 shell closure is quenched due to a weakening of the spin-orbit splitting, such as the reduction of Z=28 suggested in ^{78}Ni, the N=70 shell gap may increase. In that case, ^{110}Zr could become a spherical nucleus with closed-shell characteristics. In the later case, ^{110}Zr would replace the N = 82 ^{122}Zr as a waiting point along the *r* process path. This hypothesis is supported by (i) the unexplained dip encountered in abundance calculations when one does not consider a quenching of the N=82 shell closure in the neutron rich region and [25] (ii) independent calculations that predict ^{110}Zr as thetraedral in its ground state, with no quadrupolar shape [26, 27]. The evidence of significant shell effects in the region of ^{110}Zr could originate in the reduction of spin-orbit splitting, responsible of the N=82 shell closure. De facto, the study we propose should be connected to the shell structure of N= 82 isotones well beyond ^{132}Sn.

Recently, the ^{111,112}Zr isotopes have been produced and identified for the first time at RIBF [28]. A recent spectroscopy of ^{106,108}Zr at RIBF found hints for a deformed subshell closure at N = 64 in

Physics cases	1^{ary} beam	2^{ary} beam	I (pps)	Reaction	Time
N = 28	^{48}Ca 100 pnA	^{42}Si	24	(p,3p)^{40}Mg	6 days
N = 34	^{82}Se 20 pnA	^{54}Ca	2	(p,pn)^{53}Ca	5 days
around ^{54}Ca	^{86}Kr 100 pnA	^{53}K	0.5	(p,2p)^{52}Ar	4 days
N = 40	^{82}Se 100 pnA	^{62}Ti	20	(p,3p)^{60}Ca	6 days
Z = 28	^{86}Kr 100 pnA	^{80}Zn	60	(p,3p)^{78}Ni	6 days
in ^{78}Ni		^{79}Cu	2.5	(p,2p)^{78}Ni	6 days
N = 70	^{136}Xe 100 pnA	^{111}Nb	6	(p,2p)^{110}Zr	3 days

Table 1: Proposed physics cases with MINOS. Indicative time estimates to measure the excitation energy of the first excited 2^+ state with a statistics of about 200 photopeak events are based on the expected beam intensity, the γ-detection efficiency and typical cross sections of 0.3 mb for $(p, 3p)$ reactions and 5 mb for $(p, 2p)$ reactions.

this mass region [29]. These new information make the ^{110}Zr mass region particularly important to investigate.

2.5 Summary

In Tab. 1, we summarize the reactions mentioned in this section that could be performed with MINOS and DALI2 once the requested beam intensities are available at RIBF. Intensities are from [30].

3 MINOS

The instrument MINOS is under development at CEA Saclay with a **foreseen beam test around mid 2013**. It is proposed to do this first beam test of MINOS at RIKEN, and to associate it with the Gamma detector DALI2 for **physics experiments starting from late 2013**. A detector-test proposal will be submitted to the RIKEN PAC in due time. The proposed development is based on the experience acquired by MINOS collaboration in :

- the simulations, running, and analyzing of physics experiment;
- the design, manufacturing and operating of a large variety of liquid or solid Hydrogen targets;
- the micromegas detector technology, the gaseous detector readout electronics, and the operation of such detection systems in a variety of experimental conditions such as the running experiments CERN/Compass, CERN/CAST, and T2K ND280/TPCs.

The following part of the document is organized as follows. This section 3 details the current design of the MINOS instrument. The charged-particle detection will be performed with a cylindrical TPC surrounding the thick hydrogen target. The complete system is described : the liquid hydrogen target and its associated cryogenics system, the micromegas readout TPC and the TPC electronic readout. Realistic simulations are also described and have been used to determine the global instrument dimensions and the optimal TPC design in terms of readout plane segmentation.

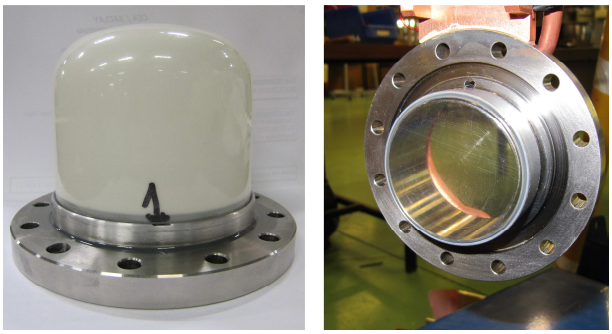

Figure 3: Picture of one of the PRESPEC target cells. (Left) Target cell with effective thickness of 61 mm. Targets from 10 to 80mm can be built in one piece of 250 μm thick Mylar. (Right) Entrance window of the target (mounted to the hydrogen circuitry system) made of 100 μm thick Mylar.

3.1 The Liquid Hydrogen target

RIKEN and CEA teams have experience in performing experiments with cryogenic hydrogen targets. Several targets have been built in both laboratories. In particular, cryogenics teams at CEA IRFU/SACM have a long experience in developing targets for nuclear-physics studies. Several targets have been developped for GSI experiments, the last in date being the PRESPEC target (see Fig. 3), and are currently recently responsible for the development of the CHyMENE target, a very thin windowless pure hydrogen for low-energy studies. More information on these targets can be found in [31].

The MINOS target cell is made of Mylar. The main dimensions are 150 mm long and 40 (56) mm for the diameter of the entrance (exit) window. The target, shown in figure 4, is divided into two parts. The first part consists of a stainless steel body with filling and return gas tubes and the mylar entrance window (125 μm thick). The second part is the mylar cell (150 μm thickness). The cap was thermoformed at 160°C by mechanical stamping, and glued to a stainless steel flange.

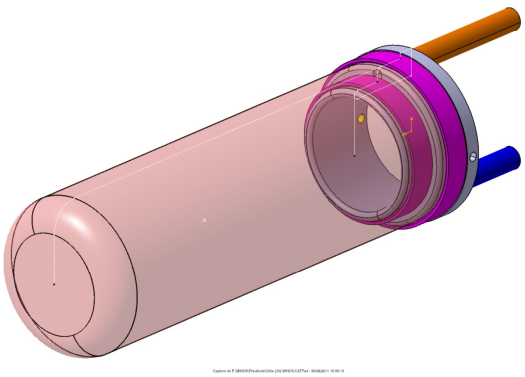

Figure 4: Details of the MINOS Liquid Hydrogen target cell. The diameter of the entrance window is 40 mm and the target length is 150 mm.

Hydrogen is cooled and liquefied in contact with the second stage of a closed-cycle refrigeration system by SHI SUMITOMO. This configuration limits liquid volume to about 100 cm^3. The target is connected to a storage tank through two separate check valves. The final pressure in the storage tank will be 1.05 bars. This eliminates all risks of explosion fueled by oxygen leaking into the system. This pressure will be the vapor pressure of the liquid, corresponding to a temperature of 20.5 K for hydrogen.

An overview of the system (composed of the target cell, the cryostat, an instrumentation bay and hydrogen tanks) is schemed in Fig. 5. A side view of the crostat+target assembly can be given in Fig. 6.

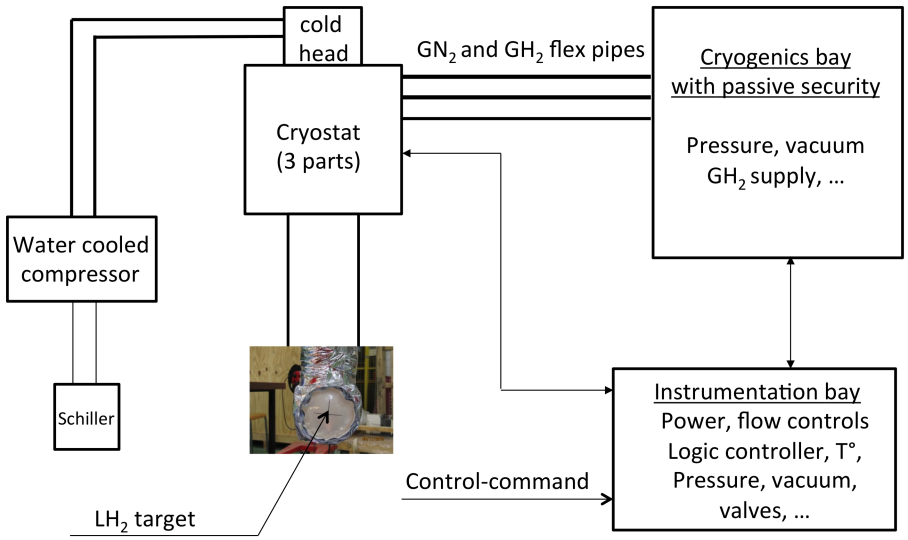

Figure 5: Overview of the MINOS cryogenics system.

The target cell is located inside a sealed vacuum chamber which provides a secondary containment volume in case of target rupture. The volume of the insulating vacuum space available for the release of hydrogen must be at least 52 times the volume of hydrogen liquid contained in the target flask since hydrogen expands 52 times as liquid is vaporized to cold gas at atmospheric pressure. The dimension of this vacuum space has been designed to limit the maximum vapor evolution rate to be vented in a target flask failure. When the target is operational, the pump is closed and vacuum is preserved by cryopumping using Actitex fabric which is more efficient than activated carbon.

The hydrogen to be used in the target will be stored in a tank of about 1000 liters. The gas pressure in the tank will be approximately 1.35 bars when all the gas is in the tank, and slightly over 1 bar when the target cell is filled.

3.2 The micromegas readout TPC

3.2.1 TPC overview and design guidelines

The tracking is essential to determine the vertex poition and therefore to allow the use of a very thick target. The trajectories of protons will be analyzed using a cylindrical Time Projection Chamber (TPC). The TPC will surround the target and be 300 mm long to access the detection of particles

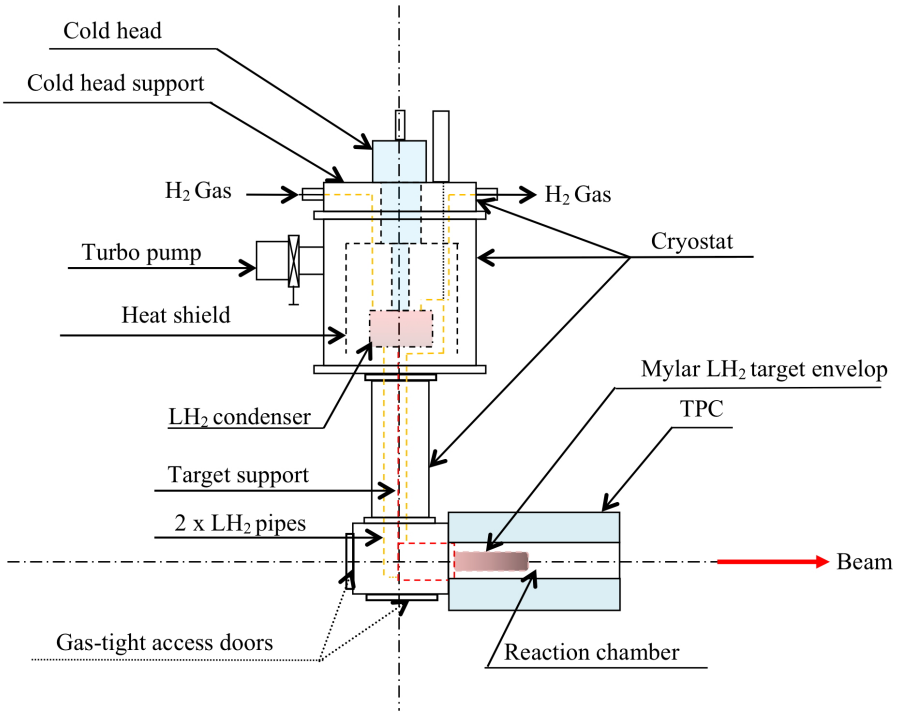

Figure 6: The MINOS liquid hydrogen target ensemble composed of a cryostat and a target cell.

emitted at small angles (see a schematic view in Fig. 7). In the case of (p, pn) reactions, it corresponds to the detection of the unique recoil proton and the projectile-like residue whereas in the case of $(p, 2p)$ reactions the projectile-like residue can be detected in coincidence with up to two protons.
Drift electrons will be amplified on the backplane of the TPC through a Micromegas amplification stage[32]. Charges will be induced on a pixelized readout plane with pads of the order of 2-4 mm^2. Signals will be digitized via a specic electronics and readout based on the GET[33] (General Electronics for TPCs) developments, a collaboration between CEA-IRFU, IN2P3 and MSU/NSCL.

The MINOS TPC design should cope with the following guidelines :

- dimensions must fit the RIKEN/RIBF+DALI2 integration constraints and the general mechanical design has to minimize material radiation length $\frac{x}{x_0}$ and optimize the resolution on the reaction vertex position in the target;
- the TPC electric field cage will be designed to optimize the fiducial volume for track reconstruction by minimizing dead zones and non-uniform electric field regions;
- the readout plane segmentation will be a trade-off between resolution performances and number of electronic channels (integration issues and cost);
- the gas mixture definition is crucial and it will be adapted to the use of the GET electronics readout features, to the readout plane segmentation, and to its gain capabilities.

The TPC field cage design is planned to start very soon (electric field lines simulations, mechanical design). A maximum 10 kV high-voltage limitation was fixed to avoid the specific

integration constraints of a higher voltage due to the needed larger insulation distances which will affect the dimensions of connectors, cables and field cage panels. The current baseline design is a self supporting cylindrical Printed Circuit Board, 100 to 200 μm thick, with about a hundred of 2.5 mm wide strips, spaced with a 3 mm pitch.

The following sections present the current status of the TPC development.

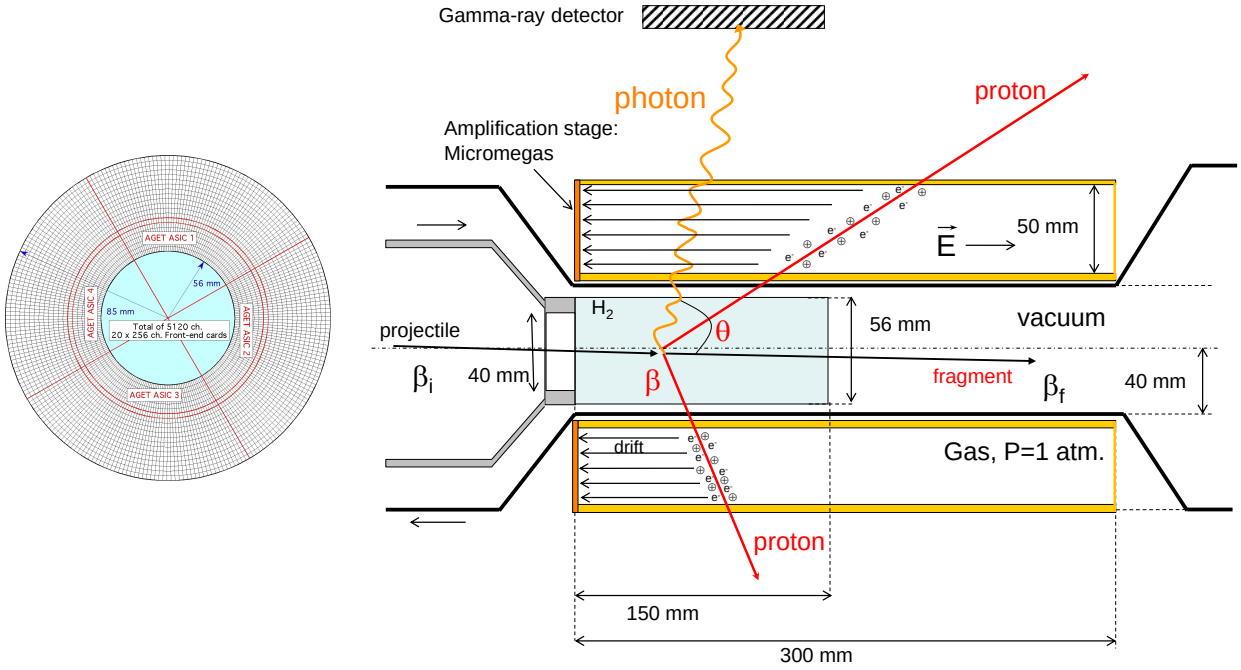

Figure 7: Scheme of the MINOS target-TPC device, as imagined today. The final vertex position resolution is intended to be lower than 3 mm FWHM. The tracker allows to measure with precision the emission angle θ and the velocity β of the fragment at the vertex position, essential for a good Doppler correction. The segmentation of the bulk micromegas readout plan of the TPC is shown on the left of the scheme.

3.2.2 The micromegas detector

The Micromegas Detector was invented by I. Giomataris, G. Charpak, and collaborators in 1995 [32]. The principle (fig. 8) is very simple : the gas volume is separated by a thin micromesh in two regions, one where the organization and drift of the electrons occurs and one, 100 micron thick, where the amplification takes place. In the amplification region, a high field (40 to 70 kV/cm) is created by applying a voltage of a few hundred volts between the mesh and the anode plane, which collects the charge of the avalanche. The anode is segmented into strips or pads.

The advantages of Micromegas is due to the amplification gap and the configuration of the electric field (fig. 8) on the two sides of the mesh, itself depending on the mesh pitch. The gap being very small, the size of the avalanche and hence the signal rise time are very small, leading to an electron signal of a few nanoseconds and an ion signal less than 50-100 ns, for most of the gas mixtures. Such ion collection allows high rates to be sustained.

The high-voltage for the drift field of the TPC will no exceed 10 kV, leading to an electrical

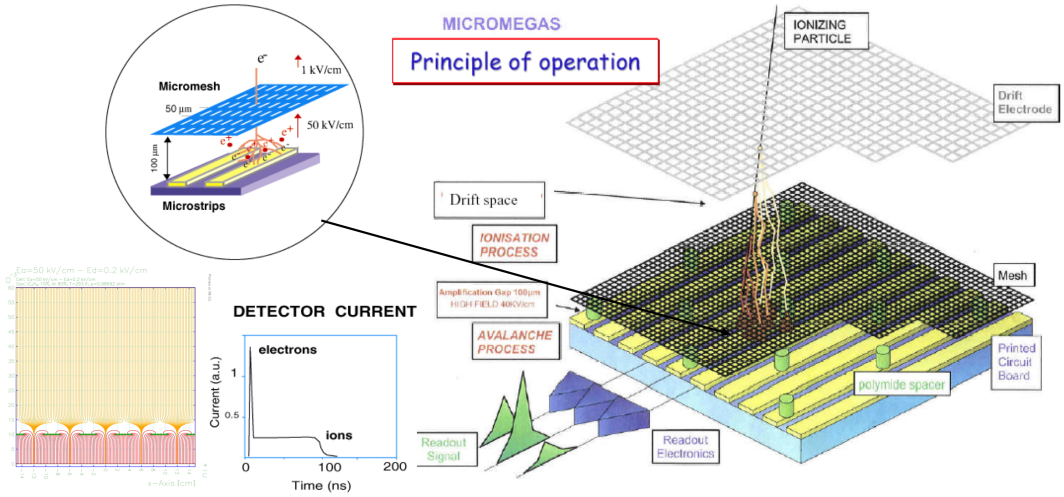

Figure 8: Schematic view of a Micromegas detector. The ionization electrons drift towards the micromesh that is placed 50-100 micron above the anode. The micromesh is supported by short cylindrical pillars. Between the mesh and the anode, here segmented to form strips, an avalanche is produced. The time structure of the signal is shown at the bottom.

potential of about 300 V.cm^{-1}. In order to achieve a rather fast drift of the electrons with a moderate longitudinal and transversal diffusion of the electrons, we propose to use the Ar-CF_4 (15%)-C_4H_{10} (3%) gas mixture (see Table 2). A 128 microns gap bulk micromegas gain was measured to be 2000 for a mesh voltage of 490 V with that gas mixture.

Table 2: Drift properties of the Ar-CF_4 (15%)-Isobutane (3%) MINOS TPC baseline gas mixture. The transverse and logintudinal diffusions C_T and C_L, respectively, are given in μm as a function of the square root of the drift distance (in cm).

gas	E (V/cm)	Operating Gain	v_{drift} $(cm/\mu s)$	$C_T/\sqrt{cm}$ (μm)	$C_L/\sqrt{cm}$ (μm)
Ar-CF_4 (15%)-iC_4H_{10} (3%)	250	2000	6.6	195	186

3.2.3 The readout plane design

The design of the readout plane is conceptual and it will depend on the final specifications of the TPCs. We propose to use the baseline design of the T2K/TPC bulk-micromegas with a 128 μm amplification gap [34, 35]. A bulk-micromegas readout plane prototype for MINOS is currently produced with these specifications (see Fig. 9). Following the results of these tests, a pad plane segmentation will be set (an option is shown on the left part of Fig. 7).

3.3 Readout Electronics and Data Acquisition

The TPC of MINOS will be composed of about ∼5000 channels fitted on a ∼20 cm diameter disk-shaped Micromegas detector plane. To reach the desired precision on vertex reconstruction, it is estimated that up to 500 sampling points per channel will be needed. The target event acquisition

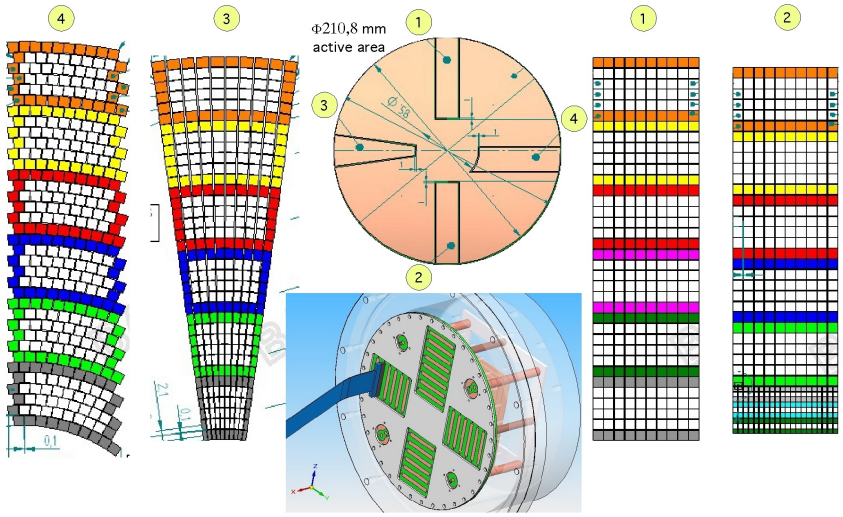

Figure 9: MINOS 2011 readout plane prototype with 4 different pad shapes and distributions.

rate is up to a few kHz. The readout electronics is not required to have specific radiation and/or magnetic field tolerance but space close to the detector plane is extremely limited. We think that all these requirements can be met by a readout system based on the AGET chip recently designed at IRFU in the framework of the GET[1] project. AGET is the evolution of the very successful AFTER chip [36] which is used for the readout of the TPC and FGD detectors in the T2K experiment at J-PARC. A block diagram of the AGET chip is shown in Fig. 10. The first silicon was produced in 2010 and is fully functional. Complete chip characterization is underway.

The AGET chip comprises 64-channels, each of these is composed of a charge sensitive pre-amplifier (four ranges from 120 fC to 10 pC), a programmable peaking time shaper (sixteen values from 100 ns to 1 ∼s), and a 512-time-bin Switched Capacitor Array (SCA). The write operation in the SCA runs at up to 100 MHz while digitization takes place at 25 MHz using an external commercial ADC. Significant dead-time reduction with AGET compared to AFTER is achieved by digitizing only those channels that were hit. Each channel also includes a programmable threshold discriminator. The outputs of all discriminators are combined on-chip. This feature can be used locally for self-trigger and it can provide a primitive for sophisticated trigger schemes in active target TPC applications. The TPC of MINOS will however rely on an externally provided trigger.

The cards housing the AGET chips will need to be placed upstream the detector assembly, several tens of centimetres away from the TPC pad plane. Fine pitch, zero-insertion force, solderless, grid-array connectors coupled to flexible multi-layer PCB extenders will be used to establish connection between the detector and the front-end cards. Successful deployment in several other projects (NEXT, ForFire) of Micromegas detectors readout via 200/300-contacts, GFZ series connectors from [2]Samtec coupled to 100 μm trace / 100 μm conductor spacing flexible Kapton extenders gives us confidence that this technology is also adequate for MINOS. Validation of the various elements in a prototype setup is being planned and we foresee that the approximately twenty 256-channel front-

[1]The GET project is building new Generic Electronics for TPCs. Developments, partially funded by French National Research Agency (ANR) involve CENBG (Bordeaux), IRFU (Saclay), GANIL (Caen) and NSCL (Michigan, USA).

[2]http://www.samtec.com

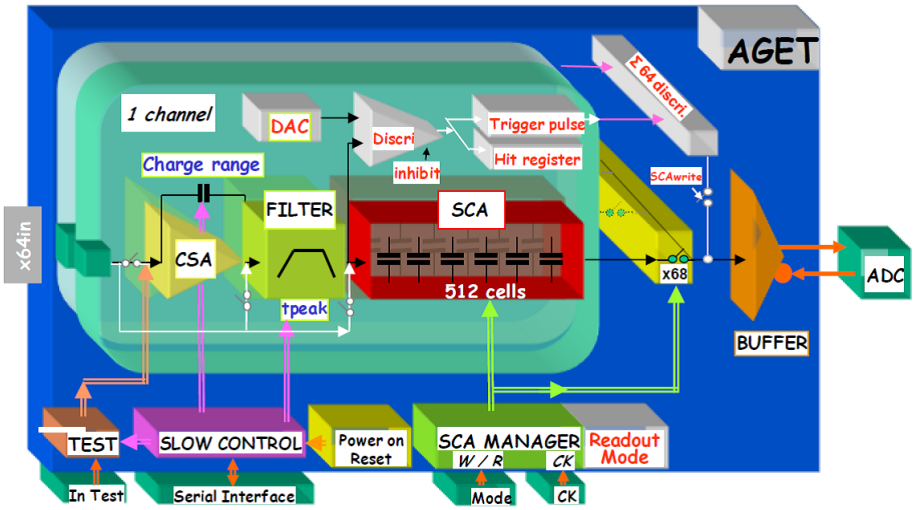

Figure 10: Block diagram of AGET.

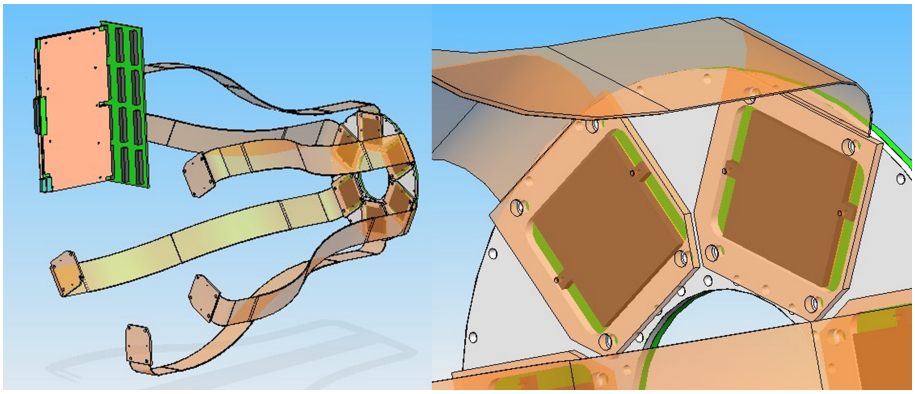

Figure 11: Conceptual design of TPC plane to front-end electronics interface.

end cards that are required can be connected to the TPC pad plane via a set of six 900-contact, ∼50 cm long flexible extenders, or a larger number of lower density assemblies (e.g. fourteen 400-contact connectors and flexible assemblies). A preliminary drawing of a possible arrangement is shown in Fig. 11. The total power dissipation of the front-end electronics is expected to be ∼200 W. No specific cooling besides air blowers will be required.

The baseline design of the TPC readout system uses as many as the components that will be made available through the GET collaboration. These include the AGET chip, the 256-channel AsAd front-end card, the 1024-channel CoBo back-end card, the clock and trigger Mutant board, and the overall DAQ software framework. A fall-back solution based on existing T2K front-end cards (equipped with the AFTER chip) or newly produced front-end cards upgraded with AGET is studied independently. The final decision between the two options will be made in 2012, after the proof-of-principle of complete working chains scalable to the size required for MINOS has been shown, and performance, cost, technical risks, and production timescales of the two candidate schemes have been assessed and reviewed.

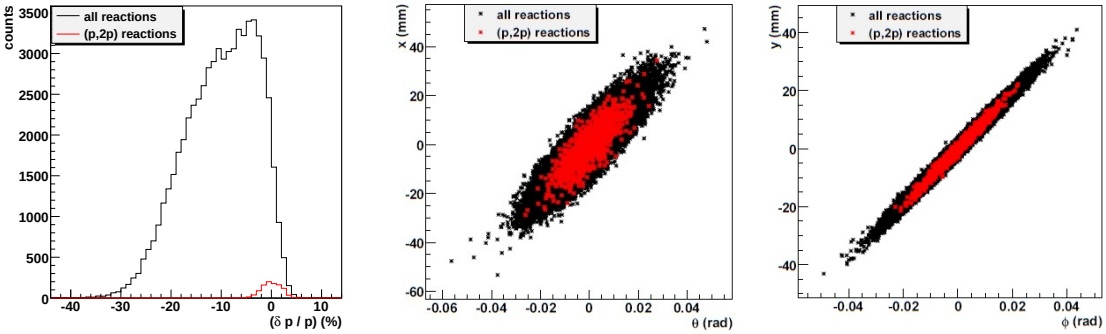

Figure 12: (Left) Momentum dispersion of the residual nuclei from reactions of ^{53}K in the liquid-H_2 target (in black). The relative distributions are centered on the momentum of ^{52}Ar fragment, producted by $(p, 2p)$ reaction, which figures in red. (Middle) Emittance of the residual nuclei relative to the horizontal plane. (Right) Emittance of the residual nuclei relative to the vertical plane.

3.4 Simulations

Over the past 4 months we have developed a simulation code based on GEANT4 [37]. Preliminary results are presented here for a realistic beam of ^{53}K interacting with the target. Reactions of spallation are studied and especially (p,2p)^{52}Ar reactions for which the resolution on the vertex has to be measured. Simulations have been playing an important role to evaluate the performances of the setup, the chosen geometry and technical solutions.

The simulations include reaction cross sections and kinematics from the INCL4 code [38] to simulate spallation reactions. A beam of ^{53}K is generated in the liquid-H_2 target. The characteristics of the beam, in terms of spatial extension, energy and momentum distributions, follow those determined with the LISE++ code [39] at the BigRIPS separator of RIKEN from a ^{86}Kr beam at 350 MeV/nucleon fragmented onto a ^{9}Be target. At the secondary target, the ^{53}K energy is 253 MeV/nucleon.
For the simulations, the characteristics of the setup are as follows: (i) a target with a radius of 28 mm and a length of 150 mm; (ii) an aluminium chamber with a radius of 38 mm, a 2 mm thickness and a 300 mm length; (iii) a TPC, filled with a gaseous mixture of $Ar_{82}(CF_4)_{15}iso_3$, with an inner radius of 42 mm, an outer radius of 92 mm and a length of 300 mm.

With such a target thickness, a total reaction yield of 37.6% is observed. The $(p, 2p)$ reaction of interest shows a yield of 0.5%, decreasing to 0.4% when double reactions are rejected for which the daughter nucleus can not be identified.

The question of the reaction kinematics is of large importance, primarily concerning the ejectile nuclei. Indeed, the identification of the residual nuclei are needed to select the reactions of interest. Figure 12 shows the characteristics of the residual beam at a distance of 1 meter after the entrance window of the LH_2 target. The emittance of the fragments and the momentum dispersion are shown for all the reactions and for the selected $(p, 2p)$ reaction. Due to the low angular and energy straggling in hydrogen, the final emittance is rather small and fits with acceptance of spectrometers

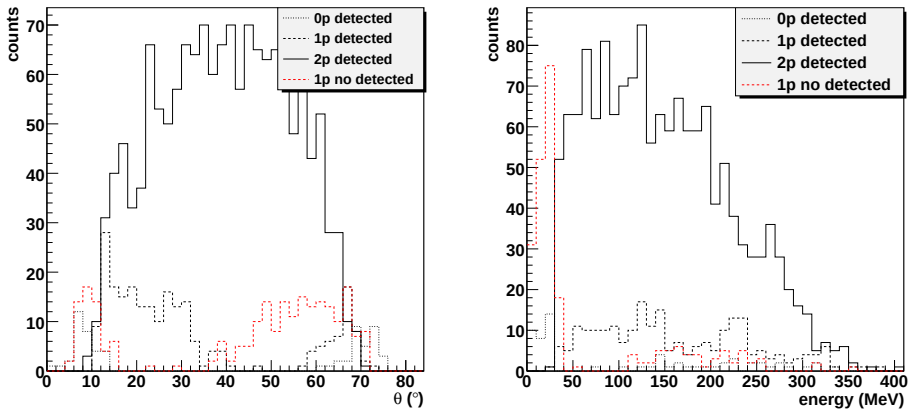

Figure 13: (Left) Scattering angle of the protons emitted from $^{53}K(p,2p)$. Selections are made when zero, one and both protons are detected. A distribution centered around 40° is observed when both protons are detected. (Right) Energy distribution of the protons from $^{53}K(p,2p)$ reactions. The undetected protons are situated at small energies or small angles of emission.

where the DALI2+MINOS setup is intended to be used at RIBF.

The detection efficiency of the TPC has to take into account relaistic kinematics of the produced protons from a $(p,2p)$ reaction. The left part of figure 13 shows the angle of emission of the two protons when zero, one and both protons are detected whereas the right part of figure 13 shows the results concerning the energy of emission. When both protons are detected, the angle distribution peaks at 40° for an energy between 50 and 300 MeV. When only one proton is detected, one can see that the undetected protons are essentially at small energy (below 30 MeV) and at high scattering angle (above 45°). Moreover, a small quantity of undetected protons concerns protons at very small angles (below 15°) and energy of emission between 100 and 300 MeV. An energy of 30 MeV and an angle of emission of 15° constitute limits below which the protons are not detected with hte MINOS setup. A total detection efficiency of 97% for $(p,2p)$ reactions is found, with 74% for the detection of both protons and 23% for only one proton detected. Interestingly, a detection efficiency of 100% is found for $(p,3p)$ reactions and 75% of the protons are detected for $(p,p'n)$ reactions.

Before calculating the resolution over the vertex of reaction, it seems interesting to compare the kinematics of emission of the protons for the reaction studied with a simulation for which only protons are generated in the target with varying energies and angles of emission. Figure 14 illustrates this purpose. One can see that the region of emission of the protons from (p,2p) reactions are situated in the region where the resolution expected is less than 3 mm.

The resolution corresponds to the distance along the beam trajectory between the reconstructed vertex projected on the beam axis and the emission point from the simulation. Figure 14 shows the resolution obtained at the FWHM of the spectrum, with a value of 2.8 mm, which is in agreement with the required limit of 3 mm FWHM.

In the near future, microscopic $(p,2p)$ and (p,pn) cross sections from the code THREEDEE will also be implented for more realistic estimates.

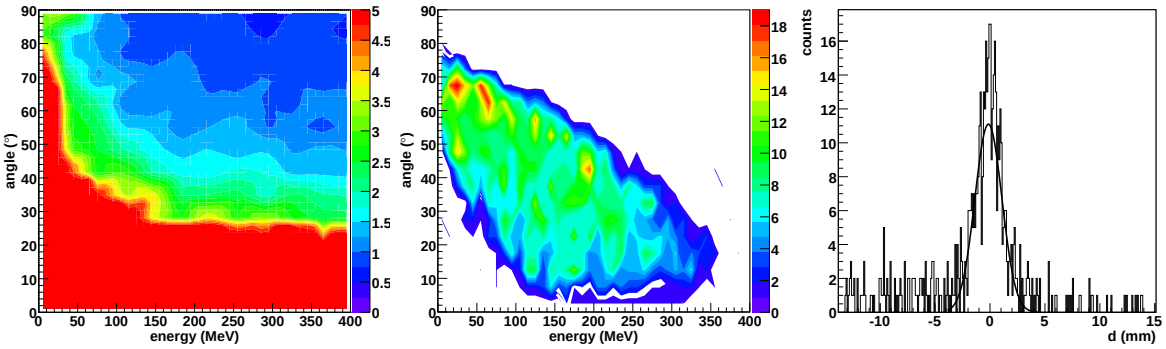

Figure 14: (Left) Resolution obtained from simulations with protons generated in the target as a function of the angle and energy of emission. (Center) Scattering angle of the protons from (p,2p) reactions on ^{53}K as a function of the energy of emission. One can see that the protons are situated in the region where a resolution below 3 mm is reached. (Right) Distance between the fitted vertex projected on the beam axis and the vertex of emission from the simulation. A Gaussian fit gives a resolution of 2.8 mm at FWHM.

4 Installation at RIKEN

We propose to use the MINOS instrument in association with the DALI2 gamma detector at RIKEN for experiments on the zero degree beam line or with the SAMURAI spectrometer.
The design of the MINOS instrument, foreseen to end in mid 2012, is therefore optimized to be coupled with DALI2. A close collaboration with the DALI2 experts was initiated at the RIKEN-IRFU workshop (RIKEN, january 2011). Since the critical path for the MINOS design is the definition of the mechanical specifications of the instrument, we focused the first studies on the mechanical integration of the MINOS instrument on the beam line, in DALI2. The current status of these studies is described in section 4.1. The requirements for the operation of the MINOS instrument at RIKEN are listed in section 4.2, in terms of fluids, electric power, and Data Acquisition. A first risk assessment and safety-related issues are finally presented.

4.1 Mechanical integration of MINOS+DALI2 at RIKEN

As described previously, the MINOS instrument part which is coupled to the beam line is composed of 2 parts : a light part ($<$ 10 kg) made of the TPC surrounding the liquid hydrogen envelop and a heavy part ($\sim$ 400 kg) made of the cryostat (see figure 15). This ensemble will be installed on the zero degree beam line in F8 vault, at $\sim$ 170 cm from the ground, in the $\sim$ 2 m space between the upstream PPAC box and the downstream Qpole (see figure 16). The DALI2 gamma detector is divided in two panels supporting the scintillators and mounted on slides. These two panels can be moved on both sides of the beam up to 60 cm apart to insert the MINOS instrument as a whole from the top (see figure 17). This operation will be done with the help of a crane supporting at least 0.5 tons. The time needed for preparation and mechanical coupling of MINOS on the beam line can be estimated to half a day.

In case of a maintenance operation on either the target or the TPC, the whole MINOS instrument including the cryostat or only the TPC+Target ensemble will be lifted from the top of DALI2. In the later case, the cryostat will be disconnected from the TPC+target part through Gas-tight access doors on either sides of the beam pipe. A small lab ($\sim 40m^2$) equipped with a class 10000 clean

Figure 15: CAD view of the MINOS instrument ensemble to be coupled to the beam line.

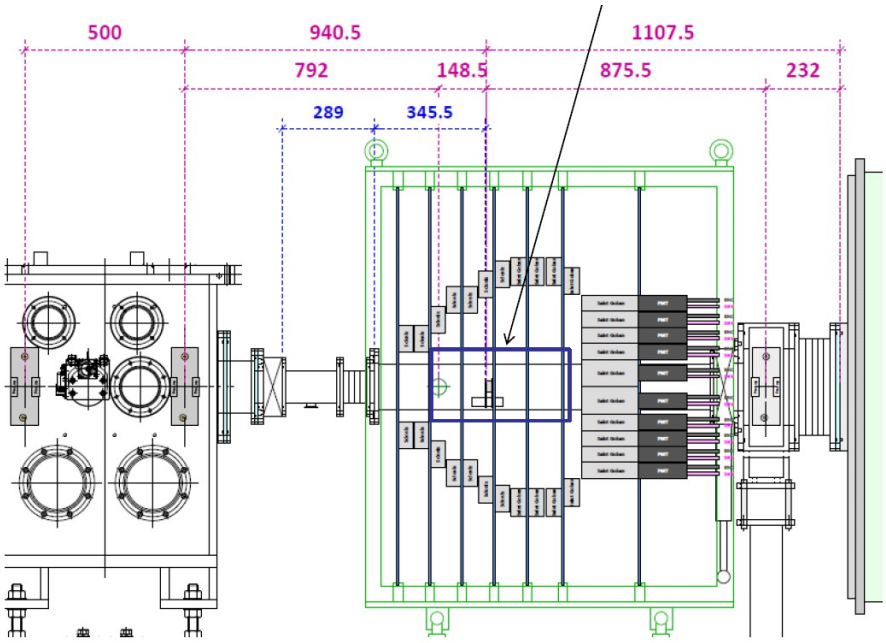

Figure 16: Side view of the F8 beam line location where the MINOS instrument could placed (inside DALI2).

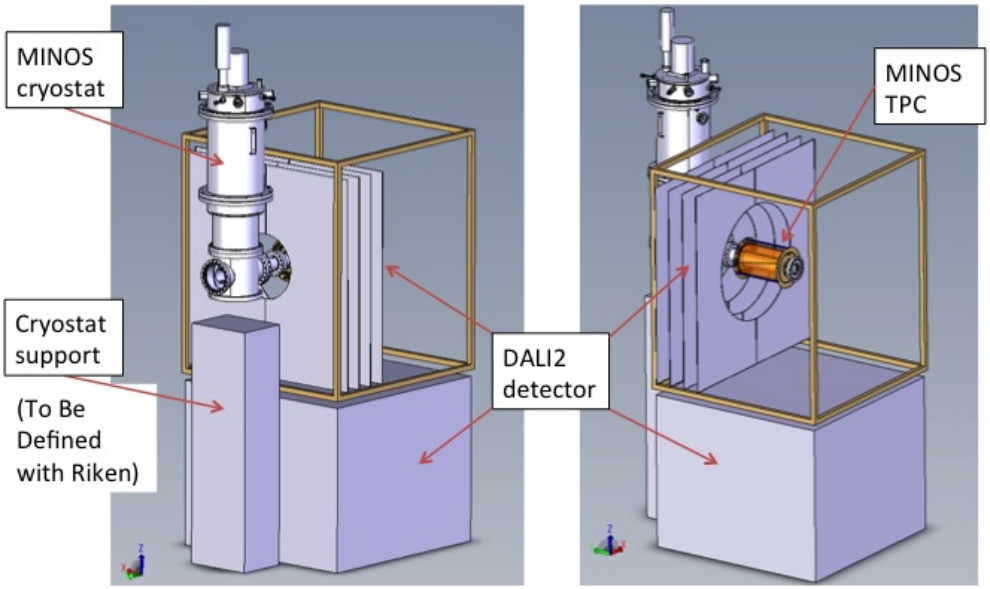

Figure 17: CAD view of the MINOS instrument coupled with DALI2. Only the external frame of DALI2 is shown with few support drawers of scintillators.

room will be needed for eventual target or TPC maintenance.

4.2 Requirements for MINOS+DALI2 operation and maintenance at RIKEN

The complete MINOS installation on the beam line, including mechanical installation, fluids coupling, high voltage and low voltage equipments installation, TPC electronics readout coupling, DAQ coupling and instrument final tests, can be estimated to at least 4 work days the first time it will be done at RIKEN.

4.2.1 Fluids requirements

A 50 liters B50 of ultra-pure hydrogen gas will be used and sufficient to operate the MINOS instrument for months of operation. This bottle may be located outside the building to cope with safety regulations. 20 degrees centigrade water must be available close to the MINOS instrument with a flow rate of 10 liters per minute.

The baseline TPC gas is Ar-CF_4 (15%)-Isobutane (3%). It is planned to use 50 liters premixed bottles at 50 bars and to fill the TPC through two inlets at both endcaps of the TPC with 10 l/h max in normal operation. The premix bottle can either be stored inside or outside of the building following the RIKEN safety regulations. TPC gas will be exhausted through dedicated pipes outside of the building (no gas recycling is planned) and the TPC operated at few mbars above atmospheric pressure. Up to 60 l/h flow rate will be used to speed up the TPC volume filling and outgassing prior to operation. The gas purity will be monitored at the output with O_2 and water analyzers at a 1-10 ppm level.
One premix bottles should be sufficient for a 7 days experiment campain. The premix bottle will be bought by the Saclay group from a japanese supplier.

4.2.2 Electrical power equipments

The Liquid hydrogen target cryogenic system will need 15 to 17 kVA to be operated. This includes the electrotechnic bays for control and command of the system. This estimate is based on the actual power requirement for the PRESPEC cryogenic target operation which is very similar to the one of the MINOS target.
For the TPC operation, the total power requirement can be estimated to 2 kVA for the 5k channels electronics readout, 2 kVA for High-voltage supplies of the cathode (10 kV) and the micromegas readout plane, and 1 kVA for the control and command equipments.

The 15 kVA power available electrical power at the F8 vault is therefore today not sufficient for the MINOS instrument operation which requiress 22 kVA.

4.2.3 Ancillary detectors

The beam particles will be tracked on an event-by-event basis with detectors (PPACs) provided by RIKEN. The MINOS device will include a Silicon stripped detector at about 20 cm downstream the target for tracking of beam-like residues.

4.2.4 MINOS+DALI2 Data Acquisition coupling to RIKEN global DAQ

The trigger of experiments with MINOS will request a time coincidence between (i) beam tracking detectors upstream the target, (ii) DALI2, (iii) a charged particle detected in the MINOS TPC and

(iv) event in the recoil spectrometer. The MINOS readout will be triggered from an external signal, most probably coincidence between (i), (ii) and (iv).

The scheme of the data acquisition system is not defined yet. The use of NARVAL as a general framework to merge data flows from MINOS, DALI2, BigRIPS and the recoil spectrometer is a possibility to be investigated. It has already been successfully used for the MUST2 campaign at RIBF in 2010.

4.3 Safety issues

4.3.1 Liquid hydrogen target system

The design and operation of the Liquid hydrogen cryogenic target of MINOS will benefit from the previous experience of the DSM / IRFU-SACM in such cryogenic targets. This especially concerns the most recent Liquid Hydrogen target PRESPEC which was installed and operated at GSI (Germany) in may 2011. The safety procedures applied for the construction, assembly, and operation of the PRESPEC target system [40] were approved by the safety division of GSI and they will be applied for the MINOS target system construction, assembly and operation at RIKEN. This includes pressure tests on specific parts of the system such as the mylar target cell and windows, the hydrogen gas storage tank, the liquid hydrogen cryostat, and safety valves.
According to the Fermilab regulations, "Storage and use of flammable gases at physics experiments", our system is classified as risk class 0 (hydrogen volume $\preceq 7.4m^3$). This still does present some risk of potential explosion, so the system has been designed to be fail-safe and constitutes a totally closed loop with two levels of containment.
The basic idea behind safe handling of any flammable or explosive gas is to eliminate oxygen and prevent exposure to any energy source that could cause ignition. The most likely source of oxygen is of course in the atmosphere and the most likely ignition sources are from electrical equipment. The following general guidelines are used for the design of the MINOS target system:

- the TPC cage (cathode, electric field cage strips, micromegas) will be properly electrically isolated from the target cell, or any other volume containing hydrogen gas;
- no valves which could open the system to air;
- each pressure monitor is spark-proof;
- the pumps used in the storage tank circuitry are leak-proof (hermetic);
- the target cell size will be design with the minimum number of gluing and assemblies;
- stress calculus will be made for the Mylar envelops and the reaction vacuum chamber, safety coefficients will be applied, and pressure tests will be made;
- the complete hydrogen gas circuit will be assembled with metallic gaskets, and helium leak tested;
- materials in contact with hydrogen gas will be properly chosen;
- the programmed automatic procedures and alarms will be extensively tested before to trust them for routine operation with no human help;

4.3.2 TPC

The TPC gas mixture, Ar-CF_4 (15%)-Isobutane (3%), is inflammable, as stated by CERN safety regulations, since argon/isobutane mixtures are unconditionally non-flammable below $\sim 3.7\%$ and the addition of CF4 should make the mixture less flammable. This mixture will be conditioned in premix 50 liters bottles pressurized at 50 bars and the gas mixture composition certified by the supplier. The output pressure will be fixed around few bars depending on the actual location of the bottle with respect to the TPC. The TPC gas volume and the associated gas pipes assembly to the premix bottle will be helium leak tested whenever it is possible. The TPC gas volume will be less than 7 liters and fresh air supply in the F8 vault should be sufficient to prevent any risk of injuries to persons by lack of oxygen in case of TPC gas volume rupture. Nevertheless, this gas mixtures being heavier than air, a simple gas sensor should be placed on the floor close to the TPC to detect any gas leak and interlock loop used to switch off TPV High voltage and gas supply.

The bulk-micromegas micromesh will be set to $\sim$500 V. The drawn current is below a few nA when no charge is amplified in the micromegas (no beam) and it should not be greater than a few μA when beam is on. A trip threshold on the power supply will be set 1-2 μA above this drawn current to limit the current in case of sporadic sparks in the micromegas gap.
The TPC cathode plane high-voltage will be close to 10 kV. The TPC, the back sides of the readout plane and cathode, and readout electronics cards will be grounded. Shielded and isolated High-voltage connectors specified for this high-voltage range will be used.

5 Current status and agenda

The MINOS project is supported the European Research Council through a 5 years FP7/ERC European grant 258567-MINOS (oct. 2011 - oct 2015) and is fully supported by the CEA / DSM-IRFU management. The first half period ("Instrument period" is dedicated to the design and realization of the MINOS instrument and the second half period ("Experiment period") to physics experiment using the MINOS instrument. The FP7/ERC funding of 930 kEuros, is shared between 645 kEuros for Investment and travels, and 285 kEuros for 5 years Postdoctoral positions.

Four divisions of CEA / DSM-IRFU are involved in the project : (i) the Nuclear Physics Division (SphN), leading the scientific part of project through the Principal investigator A. Obertelli and providing 11 men.year physicists for the 5 years duration of the project; (ii) the Electronics, Detectors, and Computing Division (SEDI), leading the MINOS instrument part of project through the project leader A. Delbart and providing 10 men.year engineers and technicians on the "instrument period" for the MINOS TPC work package; (iii) the General Engineering Division (SIS) providing 4 men.year engineers and technicians on the "instrument period" for the Mechanical design and the Slow-control of the MINOS instrument; (iv) the Accelerator, Cryogenics and Magnets Division (SACM) providing 1 man.year engineers and technicians on the "instrument period" for the MINOS Liquid Hydrogen target system.

The global schedule of the project is shown on figure 18. The main milestones of the MINOS project from 2011 to 2015 are :

- 2011 : simulations, R&D and preliminary definition of the instrument. Succesfull tests of the PRESPEC Liquid hydrogen target at GSI in may 2011, CAD design of the MINOS integration in DALI2 (june 2011), simulations of the TPC reconstruction capabilities for readout plane

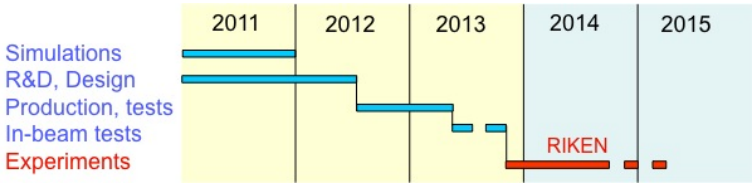

Figure 18: MINOS Global schedule.

segmentation definition (september 2011), bulk-micromegas readout plane prototype design and manufacturing and tests in 10 cm drift TPC (november 2011), start of the MINOS readout plan, TPC field cage, and Kapton flex detailed design (october 2011);

- Q1-Q2 2012 : detailed design, TPC readout plane electronics final choice based on the GET electronics (april 2012);
- Q2-Q3 2012: instrument parts production, Liquid Hydrogen target and TPC assembly and tests;
- Q1-Q2 2013 : end of TPC readout electronics production and tests, MINOS instrument final tests at Saclay;
- Q2-Q3 2013 : Liquid Hydrogen + TPC assembly, start of the TPC readout electronics production, DAQ;
- Q2-Q3 2013 : MINOS instrument validation beam tests (proposed to be done at RIKEN);
- Q4 2013 : proposed experiment with MINOS at RIKEN;

The MINOS programme based on the use of the device coupled to other detection systems such as DALI2 and zero-degree spectrometers at RIBF is open for collaborations. The use of the detector, the sharing of responsabilities from CEA Saclay and RIKEN, and an agreement on the politics for physics proposals and data sharing will be defined in a forthcoming (2012-2013) Memorandum of Understanding (MoU) between CEA Saclay and RIKEN. The device will be available for physics experiments at the end of 2013. If positively evaluated by the RIKEN PAC committee, MINOS will be considered as an ancillary detection device within the SUNFLOWER γ-spectroscopy collaboration [41] being setup in Japan.

At this very early stage of the project, the collaboration is mainly composed of teams from CEA Saclay and RIKEN (see cover page).

As a conclusion, the MINOS project is underway. The objective is to build a new device composed of a cryogenic liquid hydrogen target coupled to a charged-particle tracker dedicated to $(p, 2p)$-like reactions and in-beam gamma spectroscopy. The project is financed by the European Research Council (Starting Grant 25857-MINOS) for the period 2010-2015. We believe that the physics program to investigate nuclear structure far away from stability at RIKEN/RIBF will benefit from this new development. The coupling of the MINOS device with DALI2, in conjunction with the zero-degree or the SAMURAI spetrometers, is intended to exploit the most exotic relativistic radioactive beams produced at BigRIPS.

References

[1] J. Dobaczewski *et al.*, Phys. Rev. Lett. **72**, 981 (1994).

[2] T. Otsuka *et al.*, Phys. Rev. Lett. **87**, 082502 (2001).

[3] T. Otsuka *et al.*, Phys. Rev. Lett. **104**, 012501 (2010).

[4] J. D. Holt, T. Otsuka, A. Schwenk and T. Suzuki, ArXiv:1009.5984v2 [nucl-th] (2011).

[5] B. Bastin *et al.*, Phys. Rev. Lett. **99**, 022503 (2007).

[6] A. Gade *et al.*, Phys Rev. Lett. **99**, 072502 (2007).

[7] P. Doornenbal *et al.*, Phys. Rev. Lett. **103**, 032501 (2009).

[8] http://www.gsi.de/fair

[9] http://www.riken.go.jp

[10] D. Warner, Nature **425**, 570-571 (2003).

[11] M. Honma *et al.*, Phys. Rev. C **65**, 061301(R) (2002).

[12] S.N. Liddick *et al.*, Phys. Rev. Lett. **92**, 072502 (2004).

[13] M. Rejmund *et al.*, Phys. Rev. C **67**, 021304 (2007).

[14] T. R. Rodriguez *et al.*, Phys. Rev. Lett. **99**, 062501 (2007).

[15] O. Sorlin *et al.*, Phys. Rev. Lett. **88**, 092501 (2002).

[16] K. Langanke *et al.*, Phys. Rev. C **67**, 044314 (2003).

[17] N. Aoi *et al.*, Phys. Rev. Lett. **102**, 012502 (2009).

[18] A. Gade *et al.*, Phys. Rev. C **81**, 051304 (2010).

[19] E. Caurier, F. Nowacki, and A. Poves, Eur. Phys. J. A **15**, 145 (2002).

[20] L. Gaudefroy *et al.*, Phys. Rev. C **80**, 064313 (2010).

[21] J. Leske et al., Phys. Rev. C **71**, 034303 (2005).

[22] O. Perru et al., Phys. Rev. Lett. **96**, 232501 (2006).

[23] T. Otsuka et al., Phys. Rev. Lett. **97**, 162501 (2006).

[24] J. Van de Walle et al,. Phys. Rev. Lett. **99**, 142501 (2007).

[25] K.-L. Kratz et al., Eur. Phys. J. A **25**, s01, 633 (2005).

[26] N. Schunck et al., Phys. Rev. C **69**, 061305(R) (2004).

[27] J. Dudek et al., Phys. Rev. Lett. **88**, 252502 (2002).

[28] T. Ohnishi *et al.*, Jour. Phys. Soc. of Japan **79**, 073201 (2010).

[29] T. Sumikama *et al.*, Phys. Rev. Lett. **106**, 202501 (2011).

[30] http://www.nishina.riken.jp/UsersGuide/BigRIPS/intensity.html

[31] A. Obertelli and T. Uesaka, Eur. Phys. Jour. A **47**, 105 (2011).

[32] G. Charpak, I. Giomataris, Ph. Rebourgeard and J.P. Robert, Nucl. Instrum. Meth. Phys. Res. A **376**, 29 (1996).

[33] E. Pollacco, ANR French national Grant (2009-2012).

[34] I. Giomataris *et al.*, Nucl. Instrum. Meth. Phys. Res. A **560**, 405 (2006).

[35] A. Delbart *et al.*, Nucl. Instrum. Meth. Phys. Res. A **623** (2010) 105.

[36] P. Baron *et al.*, IEEE Transactions on Nuclear Science, volume N55, issue 3, part 3, pp. 1744 1752, June 2008.

[37] S. Agostinelli *et al.*, Nucl. Instr. Meth. Phys. Res. A **506**, 250 (2003).

[38] A. Boudard *et al.*, Phys. Rev. C **66**, 044615 (2002).

[39] D. Bazin *et al.*, Nucl. Instr. Meth. Phys. Res. A **482**, 314 (2002).

[40] J-M. Gheller, "Safety report for PRESPEC Target installation in GSI", internal DSM / IRFU-SACM note IRFU/SACM/LCSE/01JMG, march 2011.

[41] http://ribf.riken.jp/∼takesato/gamma